



Agilent EEsof EDA

Overview on Microwave Switched VCO with Microstrip Branch Resonator

This document is owned by Agilent Technologies, but is no longer kept current and may contain obsolete or inaccurate references. We regret any inconvenience this may cause. For the latest information on Agilent's line of EEsof electronic design automation (EDA) products and services, please go to:

www.agilent.com/find/eesof

Microwave switched VCO with microstrip branch resonator - the virtual ground in practice.

Stanislaw Alechno

The paper is intended as an entry to Eagleware Design Contest. Its goal is to describe the overall design of a special microwave VCO, as practical illustration of transmission oscillator analysis with virtual ground. Various parts of GENESYS suit (=SuperStar=, =SCHEMAX=, =LAYOUT=, =EMPOWER=, =T/LINE=) are implemented throughout the process showing powerful features of Eagleware software.

Design requirements

The VCO states important part of a special synthesizer with PLL gain compensation by means of VCO pre-steering. The method is to be described in a separate paper. Here the VCO design alone is of interest with stress put on topological transformations facilitating thorough design. The VCO application needs for several steps frequency switching, approximately regularly through bandwidth, according to a prescribed function. Medium tuning sensitivity is required with its variation of about 3 times within tuning voltage range. Particular requirements are as follow:

- center frequency 2.4GHz,
- bandwidth 200MHz,
- output power >10dBm,
- supply +5V, -5V,
- tuning voltage range -3V ÷ +3V,
- middle tuning sensitivity 10÷20MHz/V,
- phase noise <-110dBc/Hz at $f_m=100\text{kHz}$,
- switching by 4-bit control word for regular covering of the bandwidth.

The idea

The first step in design is to match the requirements with a general idea basing on experience. Here, using a microstrip quarter-wave resonator arranged with four PIN switching diodes seems to be reasonable. The diodes would be placed near shorted end of the resonator line shorting it more when switched on and so increasing the generated frequency. Initially one can try to place them by a pair at each side of the strip. But, looking more thoroughly and analyzing the resonator, it becomes evident that the mutual influence of the diodes, especially of one side pair, is significant. To reduce this influence and isolate the diodes from each other some operation on the resonator will be done. Let us cut the resonator strip along near the shorted end and fold these narrow strips perpendicularly so to get something like „T” letter. Thus we achieve the microstrip branch resonator. Now each diode pair can be located at the opposite sides of each branch and their mutual influence becomes reasonably low. At this point the general view of VCO can be presented with microstrip branch resonator arranged with PIN diodes as the heart of the circuitry.

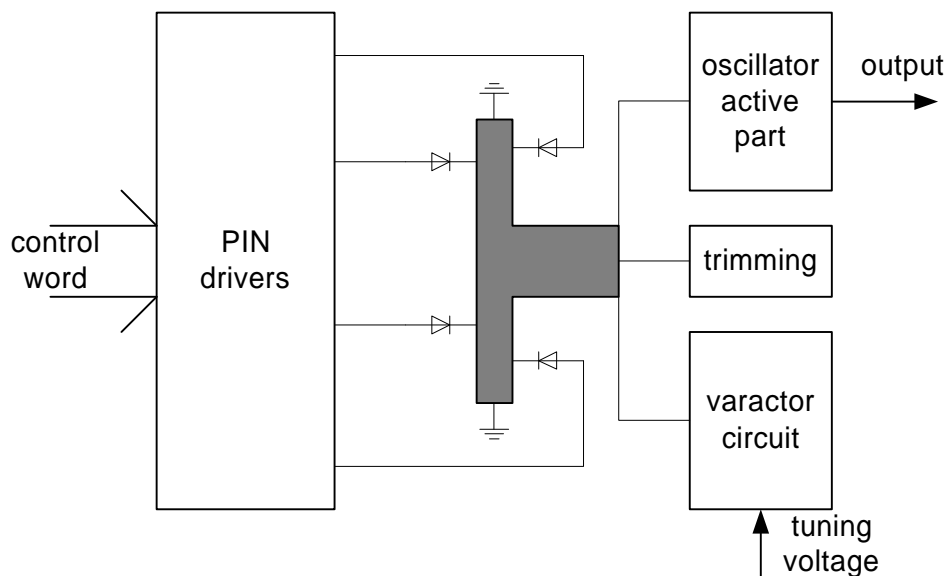


Fig.1 A general view of the switched VCO.

Having the overall design sufficiently enlighten we can direct to discuss its essential part.

The main oscillator

I am still getting surprised when browsing oscillator articles and looking as the complete and complex circuit appears suddenly. The most expensive nonlinear analysis software resolves it mysteriously giving some results but losing any insight.

I would like to show here a different approach. Starting with the basics, making fundamental transformations, seeking the very core and only then beginning simple calculations. No nonlinear software will be employed, rather universal linear simulator like user-friendly =SuperStar=, which I have been using for years, will do sufficiently.

I would like to stress, that the linear analysis states the essential part of oscillator design and the nonlinear effects can be simply taken into account at the end of the process [2]. It is important to feel all the time the relation between the computational results and the actual circuit.

Now let us focus on what I call the main oscillator. So leave behind any switching/tuning/trimming parts for a while and take the essential rest for consideration.

The most practical oscillator arrangement with a quarter-wave resonator can be drawn as simply as Fig.2a depicts: (neglecting bias elements)

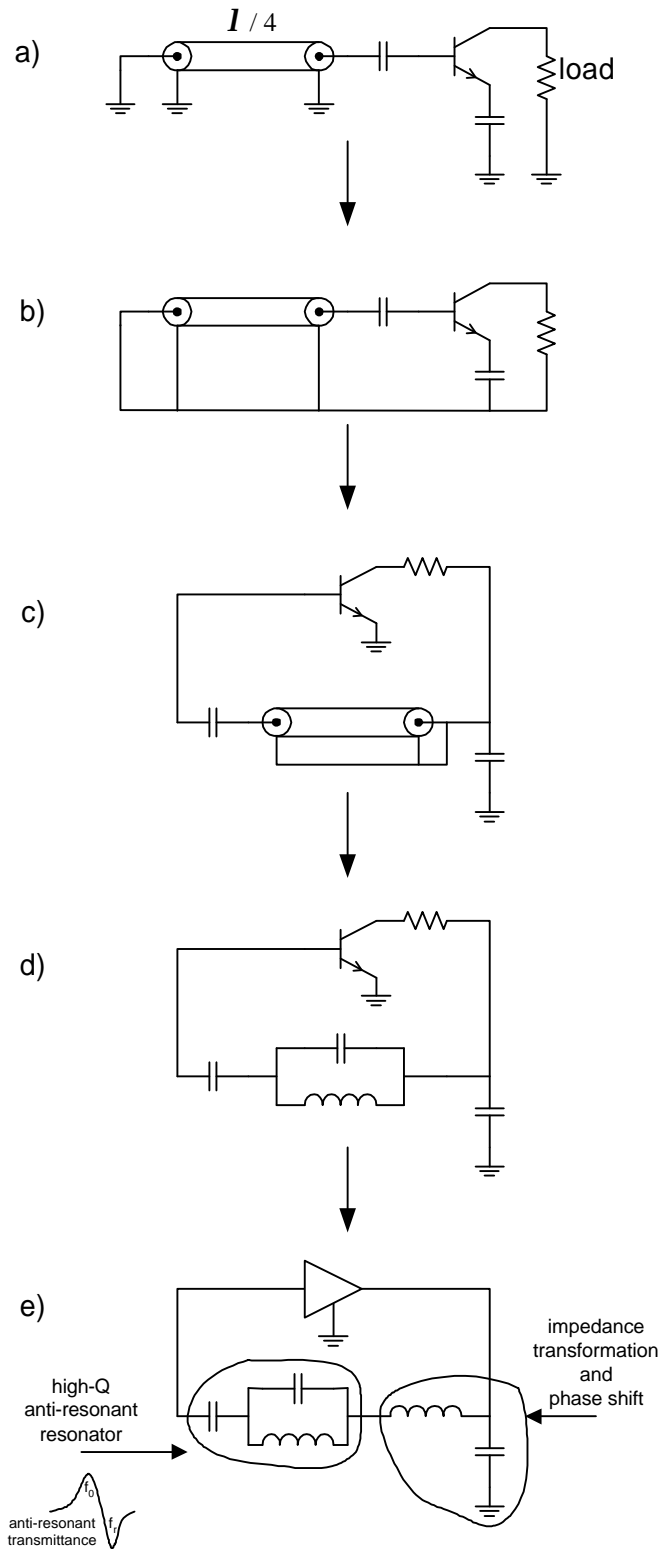


Fig.2 With the virtual ground implementation toward the core.

Next picture shows the same with float ground (or ungrounded) as the auxiliary step before the very task - implementation of the virtual ground - Fig.2c.

I am not going to describe the concept in detail here, as it was done in source [1]. The result of transformation with the virtual ground is evident - now the true oscillator loop is clear, enabling the proper insight as well as the transmission analysis. It was accomplished by placement of the virtual ground in the emitter, as usual with BJT transistors.

If someone would say that this is a useful artificial trick - I resist. It is not a mere term matter. I am reflecting on, if eventually the actual, physical ground, chosen basing on some practical but secondary reasons, should not be regarded as the artificial one. The judgement depends on criterion accepted, and this is bound with question: what is the subject here? The answer must be: it is the noise. As this is really an agent which works in an oscillating circuit. And there is always the particular point in the circuitry, which chosen as a reference shows where and how this factor acts. That is indicating how the noise is magnifying and circulating in the loop. Such a reference point truly deserves to be called as virtual or essentially true one. The actual PCB arrangement states completely different matter, tending rather to fade away the loop like in Fig.2a. The practical advantages of such implemented „artificial” ground are obvious: microstrip resonator is plainly arranged, low-inductance emitter grounding is not required, load connection is simple.

If the notion ambiguities were overdrawn a little here, it is intentionally, to face the imaginal difficulties bound with topological transformations needed in oscillator analysis. And I think, the need is just this what requires promotion.

That is enough for general comment and let us return to the actual picture as in Fig.2c. At this point one should keep in mind that such inserted quarter-wave transmission line is equivalent (neglecting higher resonances) to simple parallel resonant tank (Fig.2d) of the same resonant frequency f_r . The characteristic impedance (Z) of the lumped elements resonator is related to characteristic impedance (Z_0) of the line like below:

$$Z = \sqrt{\frac{L}{C}} = \frac{4}{p} \cdot Z_0 \quad (1)$$

And the lumped elements can be calculated from simple equations: (with $\omega_r=2\pi f_r$)

$$L = \frac{Z}{\omega_r} \quad (2)$$

$$C = \frac{1}{Z \cdot \omega_r} \quad (3)$$

Fig.2e shows already finally decomposed oscillator into three generic parts: an amplifier including the load, an anti-resonant resonator and a simple LC impedance transforming and phase shifting circuit. If it is strange how the series inductor appears, wait for a moment, it can disappear simply too. Let us focus on the anti-resonant resonator for a while because it is really the heart of the oscillator and its behavior is never revealed when such oscillators are typically calculated with negative impedance analysis. Normal characteristic of an anti-resonant resonator shown along with the schematic depicts the desired series resonance f_0 slightly below the own quarter-wave resonator frequency f_r . The actual presentation shows, what is not evident at the initial schematic. That the quarter-wave line gives transmission zero in the loop and oscillation are prompted at the slope of the notch where the series capacitor resonates out the effective inductive reactance, enabling transmission. Typically in such arrangement the generated frequency f_0 is about 5÷15% lower than f_r . It is important to keep in mind that the quarter-wave resonator (or its equivalent) does not control the oscillation freely but all depends on the series capacitance determining the working point at the notch slope, thus the generated frequency as well as loaded Q . The closer f_0 to f_r , the higher Q_L , as the equivalent reactance/phase slope gets higher. I am going to suggestion that it is hard to call the series capacitor as merely coupling one while it co-determines the working parameters. It is rather advised to take both, the parallel tank (line) and series reactance, into consideration as the whole anti-resonant resonator. Further analytical expressions will show its design in more detail. Here, I would like to notice that there are also other anti-resonant resonators as depicted in [1]. The similar form to the above, although less practical, can be achieved by using the series inductor rather than capacitor - this leads to f_0 above f_r . The same anti-resonant characteristic can be also accomplished with open-end transmission line

resonators (equivalent LC series tank) inserted in parallel into transmission path with shunt coupling reactances.

Initial calculations

Now, the inverse process to that in Fig.2, from the core - dressing with numbers - upward the final form. It is right to start from an amplifying element. For low phase noise rather a BJT would be more suited than MESFET transistor. And that should have about 10dB gain at operating frequency so to assure the minimal gain in the feedback loop of about 5dB after including every loss, mismatch and phase balance variations. Here an universal small signal microwave BJT from NEC was picked up: NE68035. It is convenient to include the load within an equivalent amplifier, like in Fig.2e. So let us insert the 50Ω load resistor (assuming no load transformation at first) into the collector branch and analyze both as our amplifier block. (The reverse influence given by S12 parameter will be neglected here for simplicity) The knowledge of its impedances is desired to start any resonator calculations. Having glance at the picture suggests that the required input impedance form is series while the output - parallel. Input amplifier impedance shows about 20Ω in series with inductance of a fraction of nH. It is always convenient to start with some pure resistive loop impedances despite that the amplifier impedances are usually significantly reactive. The practical approach is to take the amplifier reactances into consideration as additional resonator elements, usually only slightly influenced it, and to take the remained transistor resistances as the path impedances. Here, anticipating the anti-resonant resonator equivalent form near f_0 as high-impedance LC series tank, one can consider the low input transistor inductance as simply summing with the efficient series resonator inductance. Checking our amplifier output impedance we get 200Ω in parallel with 0.3pF. Here managing the capacitance is straightforward as the schematic shows it in parallel with the transforming LC circuit capacitor, simply after calculation it the value must be subtracted by 0.3pF. Thus we have achieved the path impedance starting point, when separating the loop onto an amplifier and the whole selective block, the impedance levels set by amplifier are roughly 20Ω and 200Ω respectively. So as to preserve the maximum gain margin in the loop, the required impedance transformation is 200Ω→20Ω. Calculation of the proper matching LC circuit at 2.4GHz according to expressions given in [1], yields $L=4\text{nH}$ and $C=1\text{pF}$. The sign of the reactances could be also altered but such choice like in Fig.2e is obviously more convenient. The output amplifier capacitance 0.3pF must be subtracted from the calculated capacitance so remains only 0.7pF. The calculated series inductance was delivered just to forsake it at the end, as the Fig.2 indicated, it should not figure explicitly in the real circuit. Yet, one should remember it secretly remains, simply sunk within the anti-resonant resonator, which as already anticipated, can be thought at resonance as high inductance resonated with appropriated high capacitance. Thus there is no need to make a separate series matching inductor while the resonator needs only slight correction to accomplish it.

The described simplification with series inductance should be left for final reconfiguration and now let us set the main parameters of the loop. The calculated LC pair establishes 20Ω loop impedance for further anti-resonant resonator calculations but not only - it yields some negative phase shift as well, fortunately desirable so to cancel the positive transistor phase and this way to set the proper phase balance point determining the oscillation. In the case this LC phase shifter (perceived as such at the moment) presents about -72° while the transistor about $+43^\circ$, not very appropriate values but sufficiently. It is important in engineer's action to avoid over-precision and accept relevant thresholds. In regard to phase balance two such may be taken, 30° as coarse compliance and 10° as quite close. That means for me that phase shift $<30^\circ$ at required frequency is satisfactory with initial calculation because: working near optimum resonator range is well assured, further inclusion of secondary circuit elements may be prevalent.

It is already time for some partial transmission analysis results. I would like to divide the loop for two parts at first, amplifier with transforming circuit together and remained the anti-resonant resonator alone, so to look at this more closely further. The schematic of the first part, analyzed with 20/20Ω impedances like the second, is presented in Fig.3 along with analysis results.

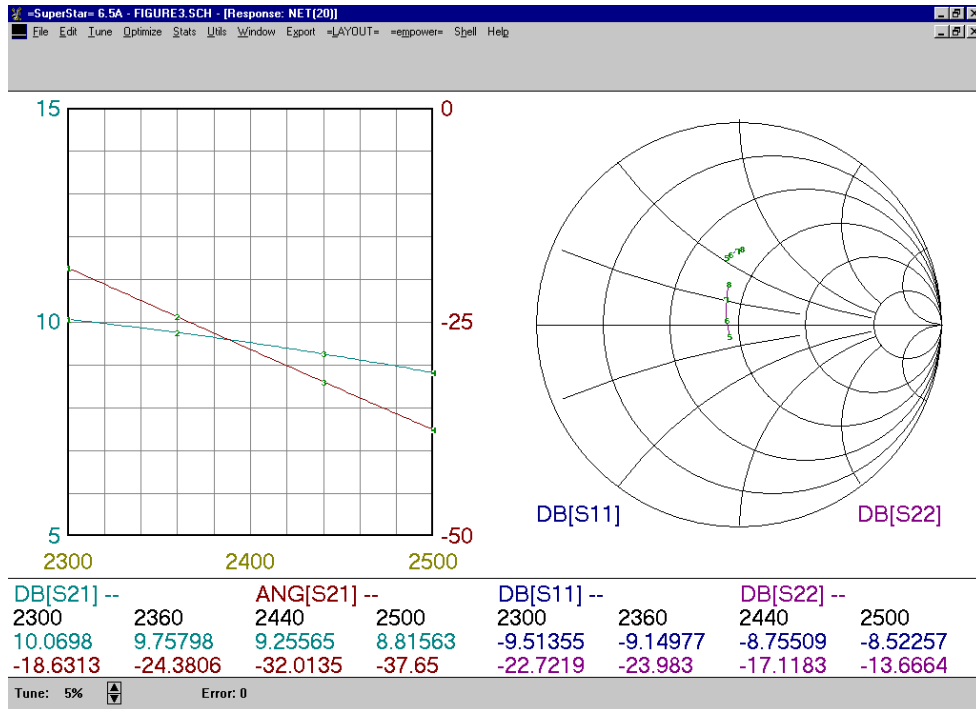
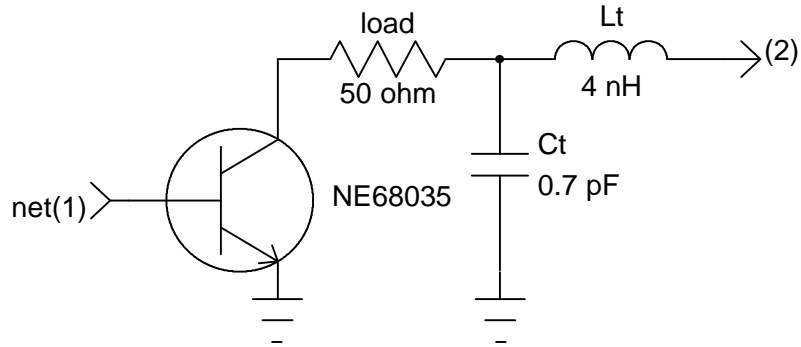


Fig. 3 The first part of the oscillator loop with its analysis results.

As the pictures show the actual gain of about 9.5dB is sufficient to leave the right gain margin in the loop while the suspected loss in the real complex resonator may reach a few dB. Rather worse input SWR, caused by the inductance noticed earlier, suggests that for more accurate results one should manage it out, for example in a manner described in [1], yet with return loss value of about 10dB it may be still overlooked.

Now it is already time to calculate the heart of the oscillator loop, an anti-resonant resonator. One essential parameter for its calculation is the loop impedance, as seen by it, here it was determined to be 20Ω at either side of the resonator. As it was already remarked such a resonator is ideally expected to deliver high-Q series resonance at desired oscillation frequency f_0 without any impedance transformation or phase shift. Its resonant frequency (actually $\omega_0=2\pi f_0$) can be simply described by lumped element values as in Fig.4, like:

$$\omega_0^2 = \frac{1}{L \cdot (C + C_s)} \quad (4)$$

The very important expression describing the resonator is that for loaded Q (Q_L). It may be presented like below:

$$Q_L = \frac{X_S^2}{X_L \cdot R} \quad (5)$$

where R - the sum of impedances terminating the resonator, here $20\Omega+20\Omega=40\Omega$, X_S - the series capacitor C_s reactance, X_L - the inductor reactance.

It is interesting equation, showing approximately direct relation to series reactance in second power but one can await that another form, function of f_r-f_0 , would be of great interest. This difference is of great significance with such kind oscillators, especially built with ceramic resonators, as a designer must first of all choose one of proper frequency, higher than f_0 , but how much?, or rather to determine if any from catalogs will work properly.

The suitable expression for exact synthesis with Q_L control is as follow:

$$Q_L = \frac{Z}{R} \cdot \frac{f_r \cdot f_0}{(f_r + f_0)^2} \cdot \frac{f_r^2}{(f_r - f_0)^2} \approx \frac{Z}{R \cdot 4 \cdot w^2} \quad (6)$$

The first form of equation (6) is terribly complicated as to calculate f_r from it, yet it simplifies greatly. One important thing to notice is that its second part shows very close approximation by 1/4, with difference <0.5% within practical range. While the second part of the equation takes simple form after introducing the useful variable:

$$w = \frac{f_r - f_0}{f_r} \quad (7)$$

The expression shows clearly the strong relation between Q_L and the relative frequency difference. The direct relation between Q_L and Z needs for comment, as simply checking it by simulator analysis indicates even Q_L degradation with Z increase. It is because the f_0 simultaneously changes, only after proportional series reactance increase, to keep the f_0 constant, the direct $Q_L(Z)$ relation is valid.

Now let us try the expressions, calculating the circuit for required Q_L . But what Q_L ? So high as possible, one can answer, as this directly influence phase noise. The real limit is stated by unloaded Q (Q_0) as when Q_L reaches it then the loop loss tend to infinity and we have only a few dB to disposal. So determining the real Q_0 at first is fundamental. Assuming initially that this is because of loss in microstrip resonator alone, its Q_0 will be derived. The laminate chosen here is RO4003 (Rogers), height 0.81mm, dielectric constant 3.38. The width of the resonator line should be rather large for high Q_0 as well as to attach all the circuitry to the resonator. Here it was chosen 5mm for main line so it will be 2.5mm for two branches of the split resonator as shown in Fig.1. Analyzing microstrip line of 5mm width in =T/LINE= we get its impedance $Z_0=24.7\Omega$ and Q_0 some below 300.

Notice please, that for comparative ceramic resonators Q_0 are not very higher. I suppose that in many cases where ceramic resonators are used arbitrarily, thorough analysis could show the implementation of microstrip line resonator as simpler, cheaper and more practical.

The previously determined Q_0 states the ceiling as to keep the Q_L well under it. For the loss we can afford, the possible Q_L can be assessed from the relation:

$$L[dB] = -20 \log \left(1 - \frac{Q_L}{Q_0} \right) \quad (8)$$

As a rule of thumb, it is reasonable to start with Q_L ten times lower than main Q_0 limitation in the circuit, thus having loss below 1dB at first. This is the first practical threshold when regarding resonator loss, with next of 3dB rather not to pass even with all secondary Q limitations. That is a normal example, sometimes at lower frequencies with lot of gain disposable one could set high resonator loss to drop it down.

According to the above, Q_L range of 20÷30 is suitable here, and that is quite high, as the standard wide-band VCO's have it about 10. With phase noise level of -110dBc/Hz at 100kHz offset to carrier typical for them, we can now expect a few dB lower value, satisfactory well enough. So the anti-resonant resonator can be calculated initially for $Q_L=20$, as it may be magnified a bit in final circuit. With this value as well as $R=40\Omega$ and $Z_0=24.7\Omega$ determined earlier one can calculate $w=0.09914$ from (6). This may confirm the rough rule-of-thumb, useful in initial assessments, to take f_r 10% above needed f_0 .

Now the desired f_r can be derived from w for our $f_0=2.4\text{GHz}$. Calculating f_r from (7) results in $f_r=2664\text{MHz}$. And further L from (2) gives 1.88nH, C from (3) gives 1.9pF, and C_s from (4) gives 0.44pF. Now the two equivalent forms of calculated anti-resonant resonator can be shown along with their analysis results, indicating close conformity one to another.

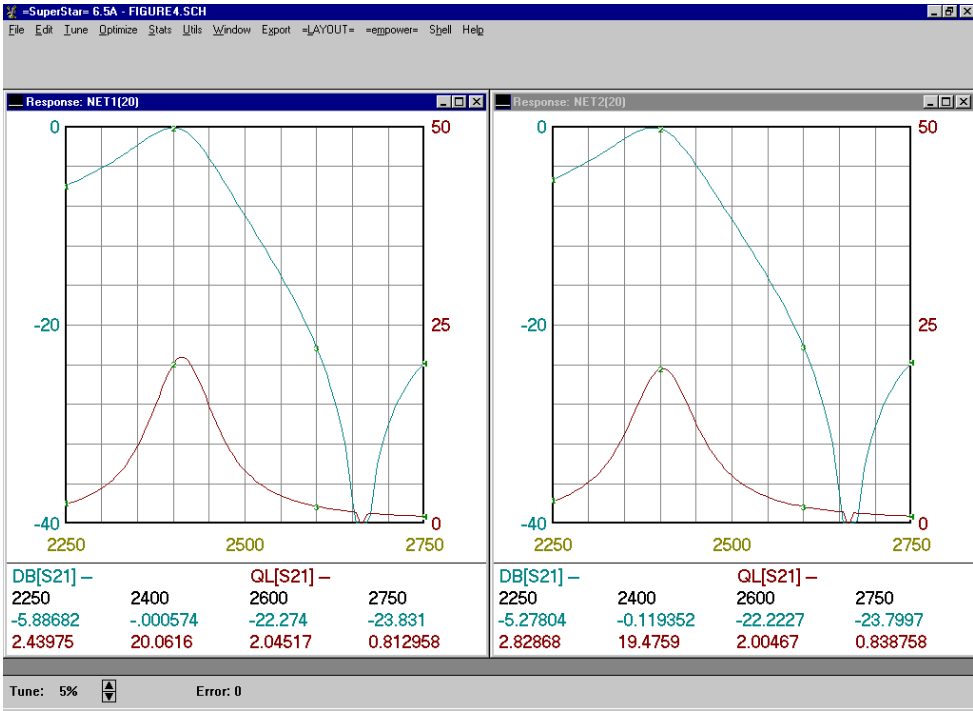
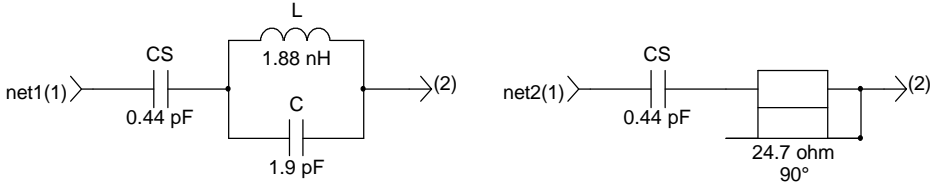


Fig.4 The second part of the oscillator loop - the anti-resonant resonator alone, in both equivalent forms, with respective analysis results.

The close agreement for analyzed lumped elements resonator confirms that simplification in (6) makes negligible difference. Small divergence in the resonator with transmission line results from limited equivalence between distributed and lumped elements circuits. Yet with such close operation near transmission line resonance like 10% the equivalence is quite sufficient.

At this moment it is already possible to analyze the complete loop transmittance as shown in Fig.5. The zero crossover point at the phase curve appoints oscillation frequency.

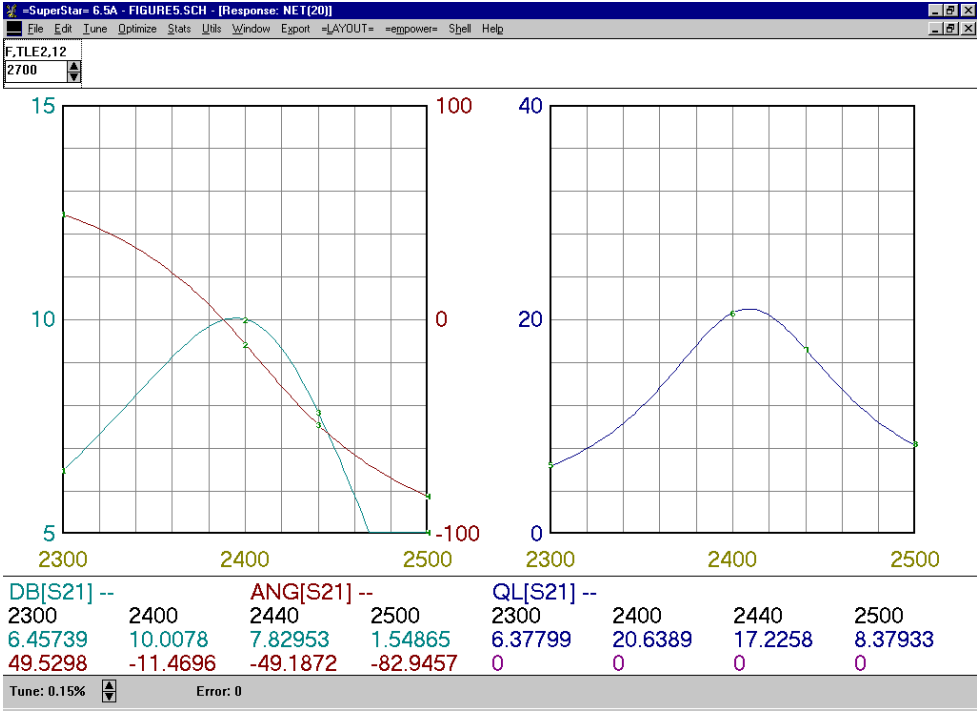
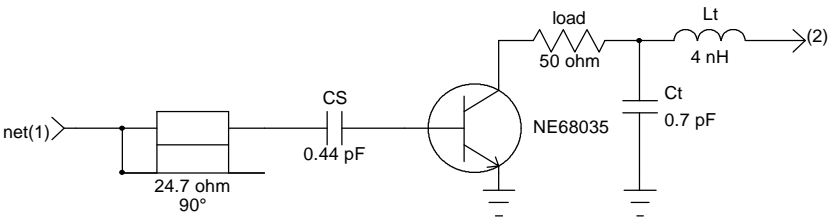


Fig.5 The overall loop transmittance for the calculated main oscillator. The resonant frequency of quarter-wave line f_r was tuned to 2.7GHz so to shift the resonance close to nominal value.

Building up

As I remarked, the goal of the paper was to emphasize that, what lacks in such kind oscillator descriptions, that is the need for topological transformations and exact synthesis of the loop. Further, what remains, is building up with all secondary parts, real models, DC components, etc. That stage, important as well as plain and tedious, may be drawn as shortly as possible.

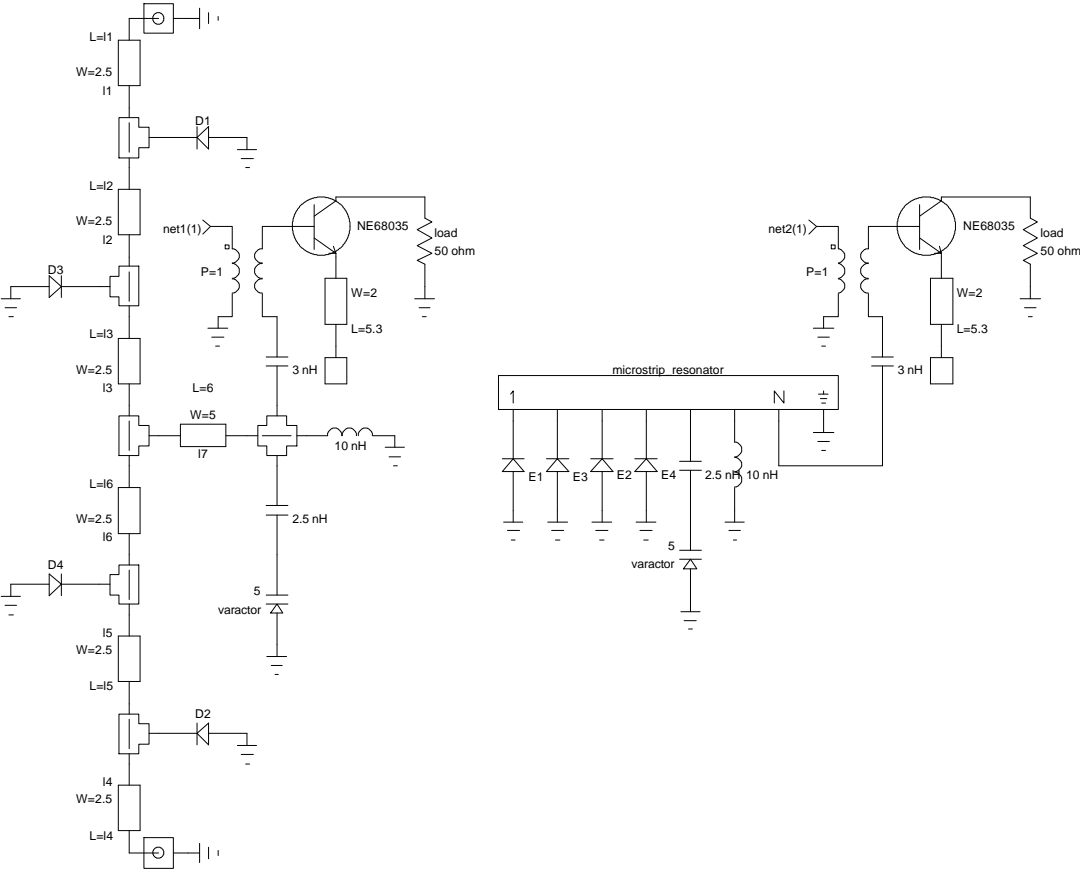
Two subsequent parts to include, the trimming and tuning circuits, can be still analyzed as extension of the approach above. An air coil connected in parallel with the transmission line resonator was accepted to accomplish fine adjusting of the generated frequency. In analyzed schematic as in Fig.5 it must be simply connected along the transmission line element. Its initial value was taken about 5 times of equivalent resonator L , that is 10nH. With its insertion the line resonator f_r must be corrected to 2420MHz so to preserve oscillation point.

Voltage tuning was accomplished with MA46H071 varactor diode (M/A-COM) in series with 1pF capacitor (3nH parasitic inductance in branch included), all in parallel to line resonator, likewise the trimming coil. The varactor diode was modeled using GENESYS built-in model. Tuning sensitivity in the

medium voltage range amounts $\sim 17\text{MHz/V}$. With insertion of the varactor circuit the line resonator f_r must be corrected to 2770MHz so to preserve oscillation point.

At this point overall loss impact was estimated by setting $Q_0=100$ for all capacitors and inductors and including transmission line loss, yielding gain margin of 8dB , already not far from the real value but one should remember it is its maximum value for optimum phase balance - rather difficult to keep while tuning and switching.

With above settlements it is time to reconfigure the circuit unto its final appearance with physical ground placed as in Fig.2a. Simultaneously the quarter-wave resonator can be transformed to its final form as microstrip branch resonator. The lately modified f_r value enables to achieve in $=T/\text{LINE}=\text{an initial length of straight line (width 5mm) resonator, of 16mm}$. This makes basis to determine initial dimensions of a branch resonator, unfolded into two branches of 2.5mm width. All the resonator structure was built of microstrip elements as shown in Fig.6 (left), so to accommodate PIN diodes arrangement as well as the rest of the circuitry:



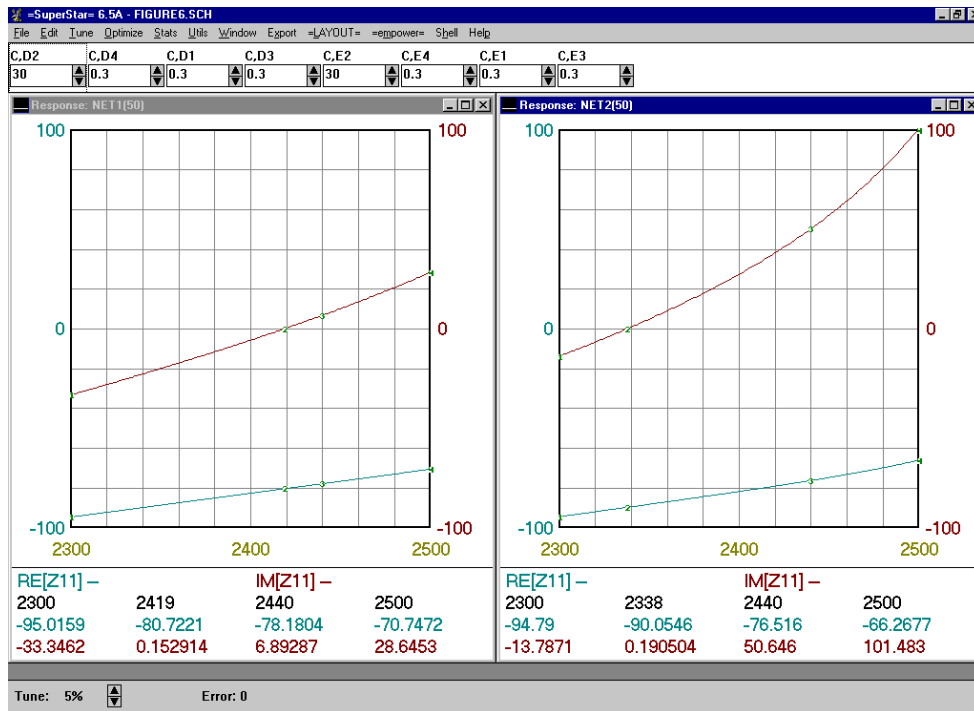


Fig.6 Final oscillator topology prepared to non-loop oscillation control. The network on left is for normal circuit theory analysis and on right for electromagnetic resonator analysis, along with respective analysis results below.

The PIN diodes applied here for resonator sections switching are HSMP 4890 (Hewlett-Packard), although cheap in typical RF case SOT 23 they were designed to achieve as low parasitic inductance as 0.75nH thus enabling their application in microwave region. Although there is a complex PIN diode model built-in GENESYS software, here for initial but insightful analysis the simplest model was used, just series RLC circuit, with $R=1\Omega$, $L=1.5\text{nH}$ and $C=0.3\text{pF}$ for OFF state altered with 30pF for ON state. The inductance includes roughly all the diode-to-ground branch inductance.

Notice, that in Fig.6 schematic the shunt capacitor $C_t=0.7\text{pF}$ was already replaced by equivalent open-end line section (2mm \times 5.3mm). That is practical solution so to avoid additional component, with its viahole as well as to make possible fine optimization of oscillation point by the line length trimming - as the previous analysis shown this modifies the phase condition directly. Besides this, such implemented open line stub may sometimes help to overcome possible undesired oscillation conditions at higher transmission line resonator resonances [1]. By the way, it is worth to remember that oscillation condition should be also additionally checked in wide range so to examine any undesired oscillations.

With current topology it is no longer convenient to proceed loop transmittance analysis but this is not necessary as well. The previous research gave just insight and main parameters estimation while now only final oscillation frequency with switching is to check. That can be accomplished with simple impedance analysis within the main oscillator branch, with help of an ideal transformer (Fig.6) as analysis probe. Resultant negative resistance serves as indication of feedback gain existing in the oscillator loop - actually invisible yet real. The zero crossover point at the reactance curve may serve to predict oscillation frequency.

Looking at the intricate geometric structure of the resonator one can suspect that standard circuit theory analysis may be inefficient with such a case. That is, evidently, the task for electromagnetic simulator like =EMPOWER=, fit especially for planar structures. Superiority of electromagnetic analysis can be depicted comparing current density distribution (Fig.7) with microstrip elements structure.

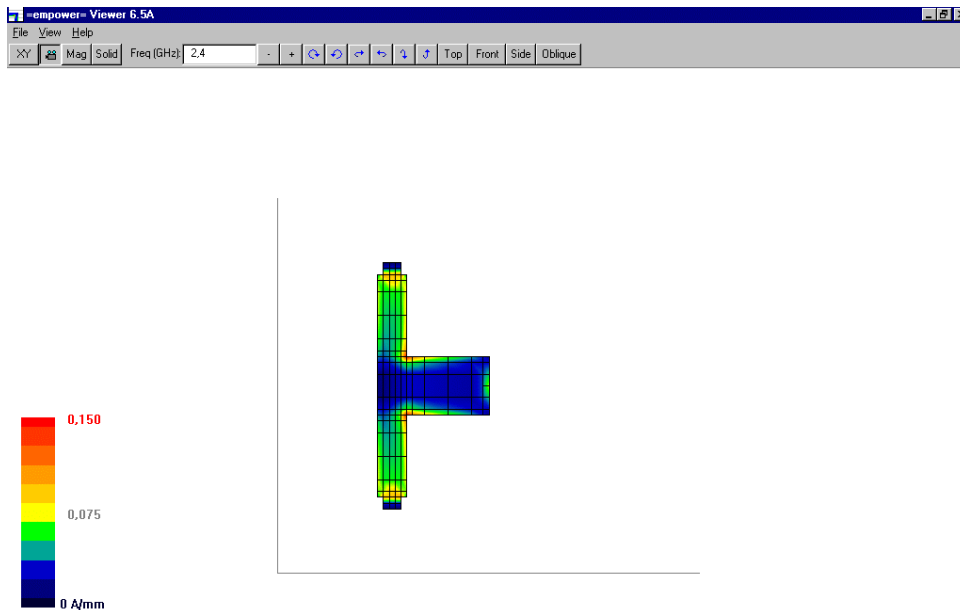


Fig.7 Current distribution across the microstrip branch resonator structure. Results for one port at the middle of the main line end.

The picture obtained from GENESYS Viewer indicates different currents at both branch edges, especially near the connection to the main line. It is expected and shows that the PIN diode action will be different when placed at opposed branch side. Obviously, such effect cannot be investigated with normal circuit analysis as for microstrip line T element its direction is indifferent.

Electromagnetic analysis in GENESYS suit is well arranged to analyze the complete PCB with fine inclusion of discrete components. But here the goal was rather to gain some insight in preliminary step, obtaining comparable results with the microstrip resonator part alone analyzed electromagnetically as shown in Fig.6 (right). The second network was created by copying the first except branch resonator elements which were analyzed in =EMPOWER= yielding a 7-port S-parameter file inserted then into the remained network. Thus the differences caused by such dissimilar approaches can be clearly checked. Anyway results are not very divergent, with differences of about 100MHz being relatively small. In practice, one can suspect that uncertainty in determining of parasitic elements may give deviations like this.

Final circuit

Figure 8 shows the final schematic with DC bias components for ~6V/20mA transistor working point and with the resonator shown as one drawing entity embedded in real switching circuitry:

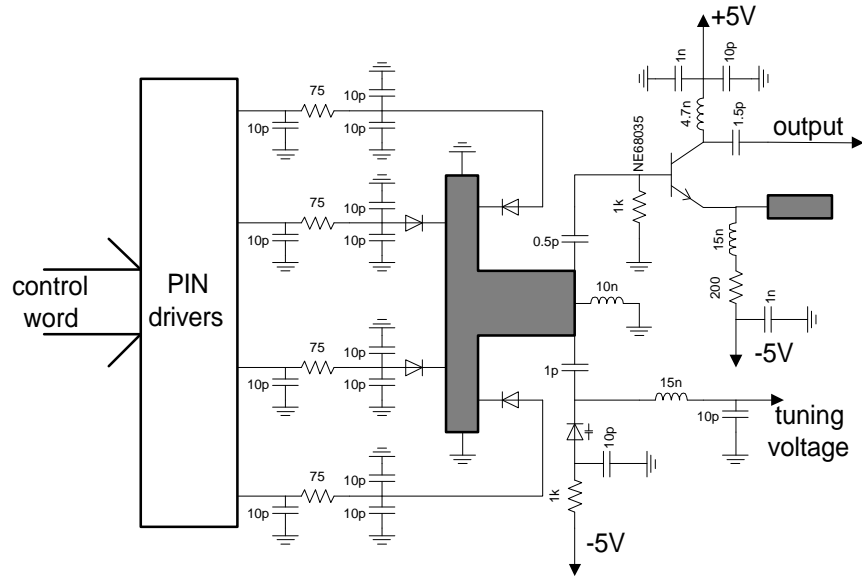


Fig. 8 The final schematic.

In the particular VCO arrangement within a special fast-switching synthesizer there was need to realize accordingly fast PIN diodes switching well below $1\mu\text{s}$. To accomplish these requirements, the PIN diodes control circuit was built on high-speed quad operational amplifier OPA 4650U (Burr-Brown). The view of real VCO model is shown at the included photo:

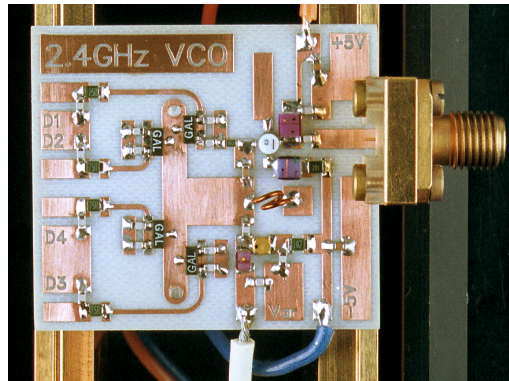


Fig.9 The view of VCO model PCB.

The VCO PCB was machined on LPKF Automill circuit board plotter. The viaholes were made with help of the riveting kit supplied with the milling machine.

Measurement of the model indicate frequency generation within required range, with output power well above needed 10dBm. Frequency switching results, before adjustments, are given in Table 1.

Control word value	1	2	3	4	5	6	7	8	9	10	11	12	13	14	15
freq. shift [MHz]	39	63	88	85	119	139	160	149	177	190	210	196	223	235	252

Tab.1 Frequency shifts achieved by PIN diodes switching, according to the value of the 4-bit control word.

Tuning sensitivity of 16MHz/V at the medium tuning voltage was measured. Phase noise below -115dBc/Hz at 100kHz offset (it is already near the spectrum analyzer HP8564E own limit) can be determined from picture in Fig.10 and harmonics, second -21dBc , third -34dBc , shows Fig.11.

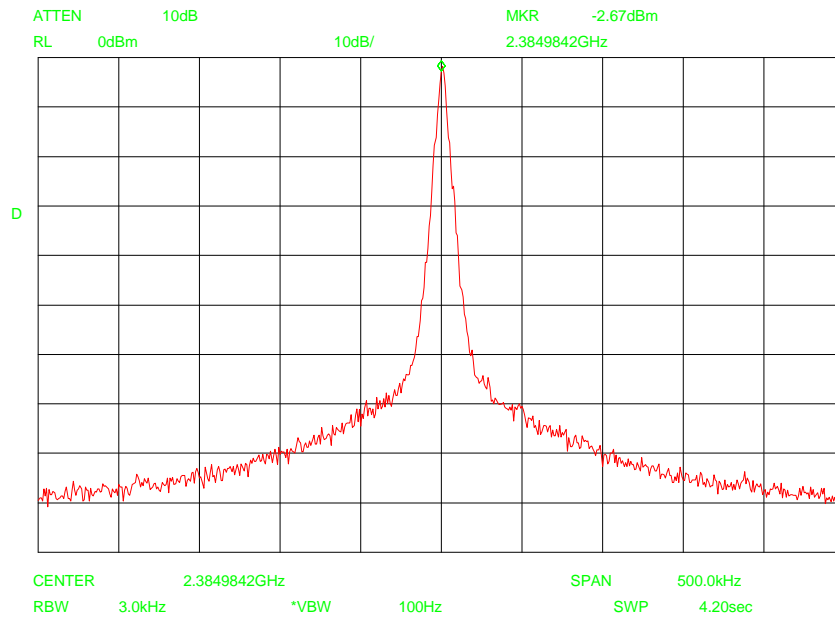


Fig.10 Output signal spectrum close to carrier.

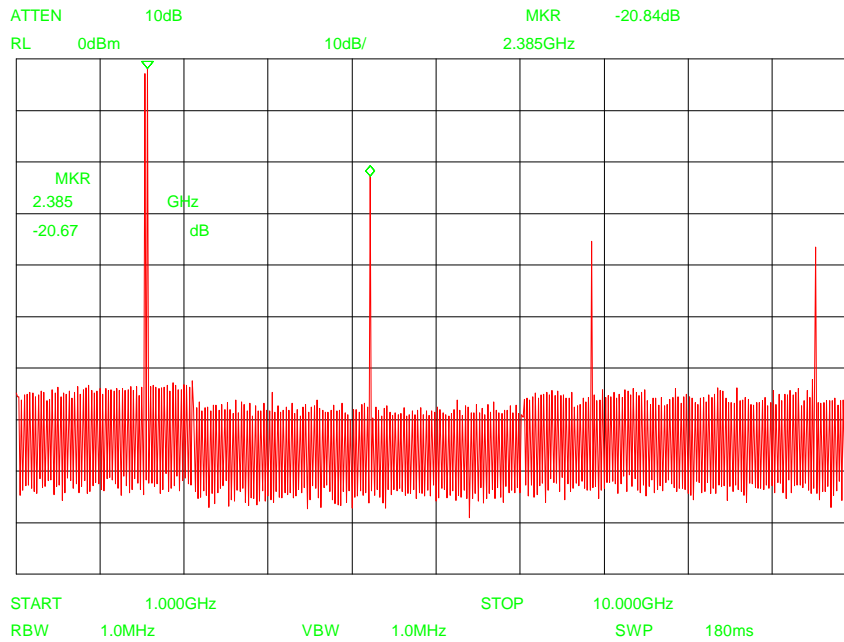


Fig.11 Output signal spectrum indicating harmonics level.

In the practical synthesizer arrangement it is required for VCO to indicate low sensitivity for enclosure proximity as well as temperature variations. Here bringing the upper metal cover down to 15mm above the PCB caused only 1MHz frequency variations while temperature increase up to ~70°C caused -5MHz frequency shift. These are quite acceptable results and comparable to expected with ceramic resonator oscillators.

Conclusions

A microwave switched VCO with microstrip branch resonator was presented as an example of virtual ground concept implementation. The need for topological transformations in oscillator analysis was emphasized with strict synthesis of the loop parts accented. Synthesis of the anti-resonant resonator structure was proceeded with practical expressions given. Finally, a real model was machined and measured indicating satisfactory agreement with analysis.

References

1. S. Alechno, „Analysis Method Characterizes Microwave Oscillators”, *Microwaves & RF*, 4 parts - November 1997 ÷ February 1998.
2. R. W. Rhea, „Oscillator design and computer simulation”, Noble Publishing, 1995.

For more information about Agilent EEs of EDA, visit:

www.agilent.com/find/eesof

 **Agilent Email Updates**

www.agilent.com/find/emailupdates
Get the latest information on the products and applications you select.

 **Agilent Direct**

www.agilent.com/find/agilentdirect
Quickly choose and use your test equipment solutions with confidence.

www.agilent.com

For more information on Agilent Technologies' products, applications or services, please contact your local Agilent office. The complete list is available at:

www.agilent.com/find/contactus

Americas

Canada	(877) 894-4414
Latin America	305 269 7500
United States	(800) 829-4444

Asia Pacific

Australia	1 800 629 485
China	800 810 0189
Hong Kong	800 938 693
India	1 800 112 929
Japan	0120 (421) 345
Korea	080 769 0800
Malaysia	1 800 888 848
Singapore	1 800 375 8100
Taiwan	0800 047 866
Thailand	1 800 226 008

Europe & Middle East

Austria	0820 87 44 11
Belgium	32 (0) 2 404 93 40
Denmark	45 70 13 15 15
Finland	358 (0) 10 855 2100
France	0825 010 700*
	*0.125 €/minute
Germany	01805 24 6333**
	**0.14 €/minute
Ireland	1890 924 204
Israel	972-3-9288-504/544
Italy	39 02 92 60 8484
Netherlands	31 (0) 20 547 2111
Spain	34 (91) 631 3300
Sweden	0200-88 22 55
Switzerland	0800 80 53 53
United Kingdom	44 (0) 118 9276201

Other European Countries:
www.agilent.com/find/contactus

Revised: March 27, 2008

Product specifications and descriptions in this document subject to change without notice.

© Agilent Technologies, Inc. 2008
Printed in USA, October 01, 1999
5989-9274EN